Available online at www.sciencedirect.com

ScienceDirect

www.elsevier.com/locate/jes

JES JOURNAL OF ENVIRONMENTAL SCIENCES

www.jesc.ac.cn

Chemical characteristics and source apportionment of $PM_{2.5}$ between heavily polluted days and other days in Zhengzhou, China

Nan Jiang, Qiang Li, Fangcheng Su, Qun Wang, Xue Yu, Panru Kang, Ruiqin Zhang, Xiaoyan Tang*

Research Institute of Environmental Science, College of Chemistry and Molecular Engineering, Zhengzhou University, Zhengzhou 450001, China

ARTICLE INFO

Article history:
Received 17 January 2017
Revised 29 March 2017
Accepted 3 May 2017
Available online 10 May 2017

Keywords:
$PM_{2.5}$
Water soluble inorganic ions
Secondary organic carbon
CMB
Back trajectory analysis

ABSTRACT

$PM_{2.5}$ samples were collected in Zhengzhou during 3 years of observation, and chemical characteristics and source contribution were analyzed. Approximately 96% of the daily $PM_{2.5}$ concentrations and annual average values exceeded the Chinese National Ambient Air Quality Daily and Annual Standards, indicating serious $PM_{2.5}$ pollution. The average concentration of water-soluble inorganic ions was 2.4 times higher in heavily polluted days (daily $PM_{2.5}$ concentrations > 250 μg/m^3 and visibility <3 km) than that in other days, with sulfate, nitrate, and ammonium as major ions. According to the ratio of NO_3^-/SO_4^{2-}, stationary sources are still the dominant source of $PM_{2.5}$ and vehicle emission could not be ignored. The ratio of secondary organic carbon to organic carbon indicated that photochemical reactivity in heavily polluted days was more intense than in other days. Crustal elements were the most abundant elements, accounting for more than 60% of 23 elements. Chemical Mass Balance results indicated that the contributions of major sources (i.e., nitrate, sulfate, biomass, carbon and refractory material, coal combustion, soil dust, vehicle, and industry) of $PM_{2.5}$ were 13%, 16%, 12%, 2%, 14%, 8%, 7%, and 8% in heavily polluted days and 20%, 18%, 9%, 2%, 27%, 14%, 15%, and 9% in other days, respectively. Extensive combustion activities were the main sources of polycyclic aromatic hydrocarbons during the episode (Jan 1–9, 2015) and the total benzo[a]pyrene equivalency concentrations in heavily polluted days present significant health threat. Because of the effect of regional transport, the pollution level of $PM_{2.5}$ in the study area was aggravated.

Introduction

In recent years, China has experienced unprecedented economic developments along with a substantial quantity of energy consumption, which results in serious air pollution problems, especially extreme haze episodes (Wang et al., 2015). A haze comprising suspended solids, liquid particles, smoke, and vapor in the atmosphere which is defined as a weather phenomenon with the horizontal visibility less than 10 km and the relative humidity (RH) less than 80% (Tan et al., 2009; Yang et al., 2015). Haze episodes have frequently occurred in China along with the characteristics of large polluted areas, long duration, and high concentration level (Wang et al., 2014b). Recently, the occurrence of haze has

* *Corresponding author*. E-mail: rqzhang@zzu.edu.cn (Ruiqin Zhang).

http://dx.doi.org/10.1016/j.jes.2017.05.006

rapidly increased in the Yangtze River Delta region and other regions (Wang et al., 2014a). Five heavy pollution episodes, whose frequencies were far greater than those in other years, were recorded in January 2013 in northern China (Ji et al., 2014).

Particular matter (PM) played a major role in the formation and evolution of haze (Tan et al., 2009). PM not only affects climate, environment, and visibility but also has a severe effect on human health (Pope et al., 2002). PM can be classified by size into PM_{10} (aerodynamic diameter < 10 μm) and $PM_{2.5}$ (aerodynamic diameter < 2.5 μm). As $PM_{2.5}$ is associated with more adverse health effects and influences on haze than larger particles (Zhao et al., 2009), numerous analyses of the haze mainly concentrate around chemistry compositions and the source appointment of $PM_{2.5}$ (Pateraki et al., 2012; Zhang et al., 2013a; Zhou et al., 2016). Sulfate, nitrate, and ammonium (secondary inorganic aerosols, SIAs) were found to be the major components of water soluble inorganic ions (WSIIs), which accounted for one-third or more of $PM_{2.5}$ (Kim et al., 2006; Cao et al., 2012; Kong et al., 2014). Organic carbon (OC) and elemental carbon (EC) are also important constituents of $PM_{2.5}$, particularly in highly industrialized and urbanized areas (Huang et al., 2014b). Elements were divided into crustal elements and anthropogenic pollution elements, including trace heavy metals harmful to the human body (Gao et al., 2015). Although polycyclic aromatic hydrocarbons (PAHs) constitute a small part of $PM_{2.5}$, they are well known to be carcinogenic and mutagenic (Hu et al., 2007).

Zhengzhou, which is the capital of Henan province, is faced with severe air pollution accompanied by the rapid development of the economy and a substantial number of people living demand, with a long-term coal-dominated energy structure (http://tongji.cnki.net/kns55/Navi/YearBook.aspx?id=N2016010114&floor=1###). According to satellite remote sensing data, China is the most serious global PM polluted area. Moreover, most of the Henan Province experienced high aerosol optical depth problems, particularly Zhengzhou (Tao et al., 2014), which is similar to the report by Luo et al. (2014). According to the data from the Ministry of Environmental Protection of the People's Republic of China (MEPPRC, http://www.mep.gov.cn/), Zhengzhou is among the 10 Chinese cities with the worst air quality in 2013–2015 and the primary pollutant was $PM_{2.5}$ (http://www.zzepb.gov.cn/Information/Content/?id=32853). Several studies have been reported on the chemical composition and source apportionment of $PM_{2.5}$ in Zhengzhou; however, only one year of data was available in most of the literature. For example, Geng et al. (2013b) determined that soil dust, secondary aerosol, coal combustion, biomass burning/oil combustion/incineration, vehicle emissions, and industrial emissions contributed approximately 26%, 24%, 23%, 13%, 10%, and 4%, respectively, to $PM_{2.5}$ mass by positive matrix factorization in Zhengzhou in 2010. A few studies on the long-term observation of $PM_{2.5}$ in Zhengzhou, such as the WSIIs, carbonaceous components (Wang et al., 2016a), and PAHs (Wang et al., 2015) of $PM_{2.5}$ were investigated in Zhengzhou from 2011 to 2013. However, the source contribution percentages were obtained during normal days excluding episodes. There was no report on source apportionment of $PM_{2.5}$ during heavily polluted days in Zhengzhou, as well as the research in long-term episode days.

In this study, 174 $PM_{2.5}$ samples were collected and WSIIs, OC, EC, and elements of the samples were detected. Chemistry characteristics and potential source percentage contribution of $PM_{2.5}$ were contrasted between heavily polluted days and other days during 2013–2015 (including a typical haze episode).

1. Materials and methods

1.1. Site description and sample collection

Zhengzhou belongs to the warm temperate zone continental climate, which has four distinctive seasons with an average temperature of approximately 15°C (http://tongji.cnki.net/kns55/Navi/YearBook.aspx?id=N2014120113&floor=1). The sampling site is located on the roof of the Collaborative Innovation Center of Henan Resources and Materials Industry in Zhengzhou University in Zhengzhou High-tech Zone (34°48′ N, 113°31′ E) (Fig. 1). The sampling height is approximately 13 m above the ground and there is no tall building around.

One hundred seventy-four samples were collected by using quartz microfiber filters (20.3 cm × 25.4 cm, Pall, USA) with a high-volume $PM_{2.5}$ sampler (TE-6070D Tisch Environmental, USA), which was accompanied by the flow rate 1.13 m^3/min during the periods from 8 December 2012 to 24 October 2015. Sampling was conducted from 9:00 am to 8:00 am of the following day.

Before each sampling, the quartz filters were wrapped in aluminum foil and baked at 450°C for 4.5 hr in a Muffle furnace. All filters were then placed in a super clean room (temperature: 25 ± 5°C; RH: 50% ± 5%) for at least 48 hr and weighed in a micro-balance (Mettler Toledo XS205, Switzerland) before and after each sampling. All filters were stored in a freezer at −20°C before analysis.

1.2. Chemical analysis

1.2.1. WSIIs analysis

Two pieces of circular membranes (each piece 10.9 cm^2) were cut from each sample filter and dipped in 25 mL ultra-pure water in 100 mL bottles. WSIIs from the samples were extracted by the ultrasonic bath for 30 min (bath temperature < 30°C). The extracted solutions were filtered with hydrophilic membranes (0.22 μm) before determination. Four anion species (F^-, Cl^-, NO_3^-, and SO_4^{2-}) were analyzed by using an ion chromatography (ICS-900, Dionex, USA) with an IonPacASll-HC4 mm anion separation column and an IonPacAGll-HC4 mm guard column. The eluents were 8.0 mmol/L Na_2CO_3 and 1.0 mmol/L $NaHCO_3$ mixtures with 0.8 mL/min flow rate. Five cation species (Na^+, K^+, NH_4^+, Ca^{2+}, and Mg^{2+}) were detected by ion chromatography (ICS-90, Dionex, USA) with an IonPacCS12A cation separation column and an IonPacCG12A guard column. The eluents were 20 mmol/L of methane sulfonic acid with 1.0 mL/min flow rate.

1.2.2. EC and OC analysis

Two 2.0 cm^2 membranes were punched from each filter and used for analysis using a carbon analyzer (Sunset Laboratory, USA). The analysis proceeds essentially in two stages. In the first, OC is volatilized from the sample in a pure helium

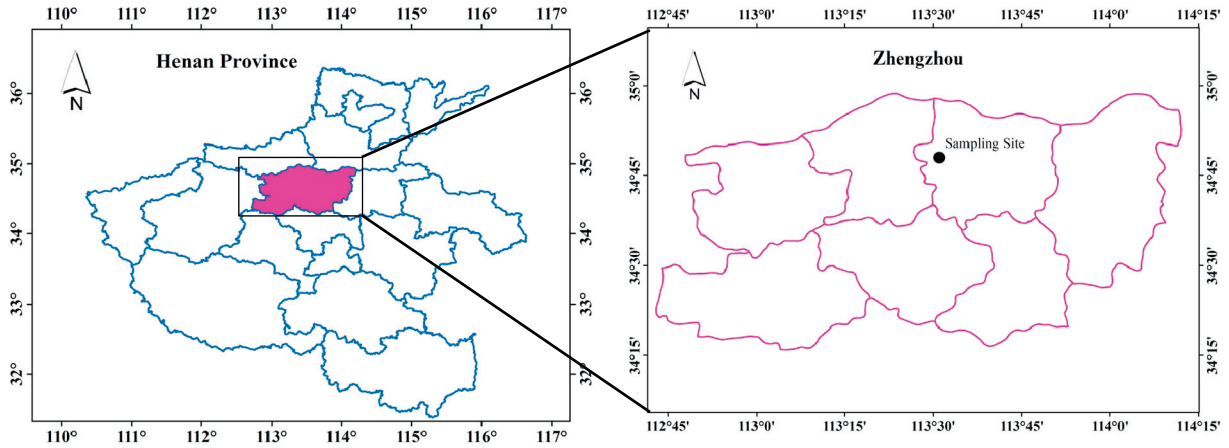

Fig. 1 – Location of the sampling site in Zhengzhou, Henan Province, China.

atmosphere as the temperature is stepped to about 840°C. During the second stage, EC measurement is made in an oxidizing atmosphere of 2% oxygen with 98% helium as the temperature is stepped to about 870°C. The carbonaceous combustion products that evolved at different temperatures were completely oxidized to carbon dioxide and reduced to methane which was detected by the flame ion detector (FID). Methane gas was used as an internal standard during the entire measurement process to calibrate the FID response signal.

1.2.3. Element analysis

Six quartz filters (10.9 cm^2 each) were placed in a high-pressure Teflon digestion vessel and were digested with a mixture of ultra-high purity acids (11.1% HNO_3/33.5% HCl), and then heated in a microwave system. The microwave system was ramped to 200°C and was retained at this temperature for 30 min. A total of 23 trace elements (Be, B, Mg, Al, Ti, V, Mn, Fe, Co, Ni, Cu, Zn, As, Se, Sr, Mo, Ag, Cd, Sn, Sb, Ba, Tl, and Pb) were measured by using inductively coupled plasma mass (Agilent 7500cx, USA) and each sample was repeated three times. Recovery as well as calibration and quantification was performed using external standard solutions, and the mixture of Li, Se, Ge, Y, In, Tb, and Bi (10 μg/mL, Internal Standard Mix) was also added for quality control.

1.2.4. PAH analysis

Six quartz filters (10.9 cm^2 each) were placed in 250 mL bottles and extracted three times with 50 mL dichloromethane and then agitated ultrasonically (bath temperature: 0°C). Each extraction step lasted 30 min. The combined extracts were filtered and concentrated in a rotary evaporation apparatus under vacuum. Sixteen PAHs, including naphthalene (Nap), acenaphthylene (Acy), acenaphthene (Ace), fluorene (Flu), phenanthrene (Phe), anthracene (Ant), fluoranthene (Flt), pyrene (Pyr), benz[a]anthracene (BaA), chrysene (Chr), benzo[b]fluoranthene (BbF), benzo[k]fluoranthene (BkF), benzo[a]pyrene (BaP), indeno[1,2,3-cd]pyrene (IcdP), dibenz[a,h]anthracene (DaA), and benzo[ghi]perylene (BghiP), which were US. Environmental Protection Agency (US EPA's) 16 priority PHA pollutants, were quantified using Gas Chromatography-Mass Spectrometry (GC–MS) (7890A GC-5975 MS, Agilent, USA) during the episode (January 1–9 in 2015) in this study. A deuterated surrogate compound mixture (Nap-D8, Ace-D10, Phe-D10, Chr-D12, and Perylene-D12) was added into all the samples for the determination of the recovery ratio. The recovery of the standard addition ranged from 79% to 104%. Only trace amounts of low molecular weight PAHs were detected in the blank filter, which was less than 5% of the amount of samples.

2. Results and discussion

2.1. $PM_{2.5}$ concentrations

The daily average concentrations of $PM_{2.5}$ and its visibility are shown in Fig. 2. As compared with the Chinese National Ambient Air Quality Standard (NAAQS) (daily standard: 75 μg/m^3), the daily $PM_{2.5}$ concentrations varied from 50 to 698 μg/m^3, with 167 days (*i.e.*, approximately 96% of the samples) exceeding the standard. The annual average values, which were 191, 185, and 150 μg/m^3 in 2013, 2014, and 2015, respectively, all these values exceeded the Chinese NAAQS (annual standard: 35 μg/m^3) with the annual mean values 3.3–4.5 times higher than the standard in three years. The annual concentration of $PM_{2.5}$ was higher than Beijing (135 μg/m^3) (Zhang et al., 2013b), Handan (131 μg/m^3) (Meng et al., 2016), and Tianjin (141 μg/m^3) (Zhao et al., 2013), as well as the southern cities in China, which were approximately 2–4 times higher than that in Shanghai (54 μg/m^3) (Geng et al., 2013a), Fuzhou (44 μg/m^3) (Xu et al., 2012), and Xiamen (71 μg/m^3) (Zhang et al., 2011). Compared with the developed countries, the annual concentration was obviously much higher with 5–13 times than Veneto, Italy (33 μg/m^3) (Squizzato et al., 2012), Yokohama, Japan (20.6 μg/m^3) (Khan et al., 2010), and Florida, USA (12.7 μg/m^3) (Olson et al., 2008). Considering the significant influence on ordinary people because of poor visibility, heavily polluted days were identified in this study by $PM_{2.5}$ daily concentrations >250 μg/m^3 and visibility <3 km.

The numbers of heavily polluted days and other days were 24 (7, 12 and 5 days in 2013, 2014 and 2015, respectively) and 150 days, respectively; the ratio of heavily polluted days is

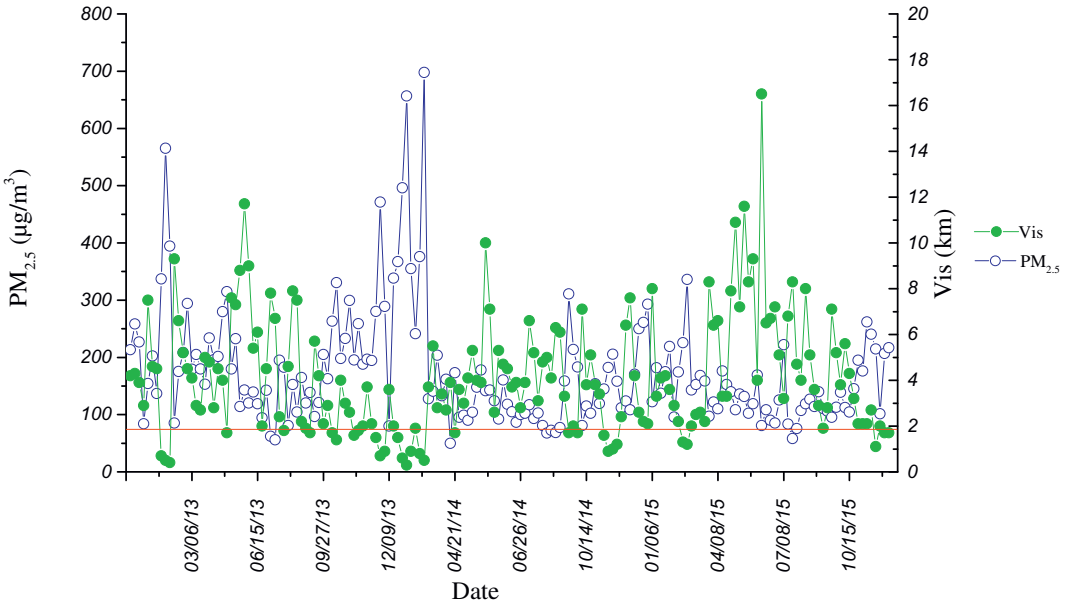

Fig. 2 – $PM_{2.5}$ daily concentrations and visibilities in 2013–2015 (mm/dd/year). $PM_{2.5}$: particular matter with an aerodynamic diameter < 2.5 μm.

approximately 14% of total sample days (n = 174). $PM_{2.5}$ mass in heavily polluted days contributed 29% of total mass of $PM_{2.5}$ from 2013 to 2015 as calculated below:

$$\text{Proportion} = \frac{\sum_1^{24} C_i * t * Q}{\sum_1^{174} C_j * t * Q}$$

where C_i and C_j represent the concentration of $PM_{2.5}$ in heavily polluted days and those in all sampling days, and t represents the time of sampling of each filter (23 hr), and Q is the flow rate (1.13 m^3/min).

The average concentrations of $PM_{2.5}$ were 366 ± 124 and 144 ± 50 μg/m^3 in heavily polluted days and in other days, respectively. The level of $PM_{2.5}$ pollution is still serious in the study area and stricter strategies should be used to reduce the pollution situation.

2.2. Chemical analysis

2.2.1. WSII analysis

The average concentration of WSIIs during 2013–2015 was 75.4 ± 48.8 μg/m^3, accounting for 44% ± 15% of $PM_{2.5}$. The ratio was consistent with previous studies in Taian (44%) (Liu et al., 2016), Wuhan (42%–44%) (Zhang et al., 2015), and Handan (45%) (Meng et al., 2016), which were much higher than that in Shanghai (32%) and Yokohama, Japan (35%) (Khan et al., 2010). The WSII concentrations in heavily polluted days and other days are shown in Table 1. An obvious distinction was observed in the average concentration of each ion and total WSIIs, which was much higher in heavily polluted days (153.6 μg/m^3) than that in other days (62.9 μg/m^3) (approximately 2.4 times), but with nearly the same WSIIs/$PM_{2.5}$ ratio (43%–44%). Therefore, the high concentration of $PM_{2.5}$ in heavily polluted days was related to the high concentration of WSIIs.

SIAs, including SO_4^{2-}, NO_3^-, and NH_4^+ were generally major ions in WSIIs (accounting for more than 80%), with the average concentrations in heavily polluted days and other days both following the order: SO_4^{2-} (55.4 and 23.8 μg/m^3, accounting for

Table 1 – Concentrations of WSIIs and carbonaceous material of $PM_{2.5}$ in heavily polluted days and in other days.

	Heavily polluted days (n = 24)	Other days (n = 150)
Visibility (km)	1.4 ± 0.7	4.6 ± 2.5
$PM_{2.5}$	366 ± 124	144 ± 50
WSIIs		
SO_4^{2-}	55.4 ± 31.8	23.9 ± 14.9
NO_3^-	41.9 ± 16.6	17.4 ± 11.7
NH_4^+	30.4 ± 14.3	12.8 ± 6.6
SIAs	127.7 ± 57.7	54.1 ± 29.1
WSIIs	153.6 ± 65.9	62.9 ± 30.9
Carbon		
OC	61.7 ± 23.3	20.6 ± 12.9
EC	12.9 ± 8.1	6.8 ± 4.1
TC	74.6 ± 23.3	27.5 ± 15.7
SOC	45.0 ± 27.2	13.1 ± 10.8
Ratios		
WSIIs/$PM_{2.5}$ (%)	43 ± 12	44 ± 15
SIAs/$PM_{2.5}$ (%)	35 ± 11	38 ± 15
NO_3^-/SO_4^{2-}	0.87 ± 0.38	0.77 ± 0.40
OC/EC	6.8 ± 5.4	3.3 ± 1.9
SOC/OC	0.68 ± 0.25	0.58 ± 0.18
TC/$PM_{2.5}$ (%)	21 ± 7	19 ± 8

SIAs: secondary inorganic aerosols (NH_4^+, NO_3^-, SO_4^{2-}); $PM_{2.5}$: particular matter with an aerodynamic diameter < 2.5 μm; OC: organic carbon; EC: elemental carbon; TC: total carbon; SOC: secondary organic carbon; WSIIs: 9 water soluble inorganic ions.
All units were in μg/m^3 unless otherwise noted.

15% and 17% of $PM_{2.5}$) > NO_3^- (41.9 and 17.4 μg/m^3, both 12% of $PM_{2.5}$) > NH_4^+ (30.4 and 12.8 μg/m^3, 8% and 9% of $PM_{2.5}$, respectively). The previous studies demonstrated that the ratio of NO_3^-/SO_4^{2-} could be reasonably used as an indicator of the importance of mobile and stationary sources to nitrogen and sulfur in the atmosphere (Xu et al., 2012; Xu et al., 2016), and high NO_3^-/SO_4^{2-} signified the predominance of mobile source over stationary source of pollutants (Arimoto et al., 1996). In this study, the ratio in heavily polluted days (0.87) was slightly higher than that in other days (0.77). Compared with other cities, the ratio was much higher than that in Fuzhou (0.41) (Xu et al., 2012), Hangzhou (0.36) (Cao et al., 2009), and Hongkong (0.26) (Pathak et al., 2003) and close to Guangzhou (0.79) (Tan et al., 2009) and Beijing (0.71) (Wang et al., 2005). However, the ratio was much lower than that in downtown Los Angeles and Rubidoux (2–5) (Kim et al., 2000) in Southern California, with low coal consumption. Overall, stationary sources in Zhengzhou are still the dominant source of $PM_{2.5}$. However, vehicle emission could not be ignored because of the rapid growth of vehicles and severe traffic jams.

2.2.2. OC and EC analysis

The mean concentrations of OC and EC in $PM_{2.5}$ are provided in Table 1, in which the concentration in heavily polluted days (61.7 and 12.9 μg/m^3, accounting for 18% and 4% of $PM_{2.5}$) was much higher than that in other days (20.6 and 6.8 μg/m^3, 14% and 5% of $PM_{2.5}$, respectively), with the annual average OC concentration of 25.8–26.8 μg/m^3 (13%–17% of $PM_{2.5}$) in 2013–2015. The annual average OC concentration was close to Shijiazhuang (26.5 ± 21.7 μg/m^3) (Zhao et al., 2013) and higher than Xiamen (three sites: 15.8 ± 9.1, 19.3 ± 9.5, and 19.7 ± 8.3 μg/m^3) (Zhang et al., 2011), Tianjin (18.8 ± 12.9 μg/m^3), and Beijing (18.2 ± 13.8 μg/m^3) (Zhao et al., 2013), and the ratios of OC/$PM_{2.5}$ were similar to those in Beijing, Tianjin, and Shijiazhuang (approximately 13%–15% of $PM_{2.5}$) (Zhao et al., 2013) and lower than that in Xiamen (25%–27% of $PM_{2.5}$) (Zhang et al., 2011). In addition, the mean OC concentration was approximately six times higher than that for Yokohama, Japan (3.8 ± 1.5 μg/m^3 or 18% of $PM_{2.5}$), with much less difference among the ratios of OC/$PM_{2.5}$ (Khan et al., 2010). The average concentration for EC was 7.7 ± 5.3 μg/m^3 during 2013–2015, which was much higher than Xiamen (three sites: 2.7 ± 1.2, 3.3 ± 1.3, and 3.5 ± 1.4 μg/m^3) (Zhang et al., 2011) and Yokohama, Japan(1.9 ± 1.2 μg/m^3) (Khan et al., 2010) and lower than Shijiazhuang (9.8 ± 4.8 μg/m^3) (Zhao et al., 2013), and the ratio of EC/$PM_{2.5}$ (5% of $PM_{2.5}$) was nearly the same as Xiamen (Zhang et al., 2011) and Shijiazhuang (Zhao et al., 2013), and lower than that of Yokohama (9% of $PM_{2.5}$; Khan et al., 2010). The average values of total carbon (TC = OC + EC) were 74.6 ± 23.3 μg/m^3 (21% of $PM_{2.5}$) and 27.5 ± 15.7 μg/m^3 (19% of $PM_{2.5}$) in heavily polluted days and other days. The results indicate that TC plays an important role in the components of $PM_{2.5}$, with a relatively substantial difference in the concentrations and a slight variation of the ratios between heavily polluted days and other days.

According to the previous study, if the OC/EC ratio exceeds 2.0–2.2, then the ratio can be used for the identification and evaluation of secondary organic carbon (SOC) (Liu et al., 2016). In this study, SOC was also found in other days as long as secondary $PM_{2.5}$ was present. As shown in Table 1, the average ratio in heavily polluted days (6.8 ± 5.4) was much higher than that in other days (3.3 ± 1.9). SOC was estimated as the following equation (Ji et al., 2014).

$$SOC = OC–EC \times \left(\frac{OC}{EC}\right)_{min}$$

where, $(OC/EC)_{min}$ was represented by the observed minimum ratio. The concentrations of SOC were 45.0 ± 27.2 and 13.1 ± 10.8 μg/m^3 in heavily polluted days and other days, respectively. The ratio of SOC/OC in heavily polluted days (0.68 ± 0.25) was slightly higher than that in other days (0.58 ± 0.18), which indicated that photochemical reactivity in heavily polluted days was more intense than that in other days.

2.2.3. Elemental analysis

Elements were divided into two groups: crustal elements including Mg, Al, Fe, and Ti (data not shown), which were considered as the main contributors to the high loading of crustal dust; anthropogenic pollution elements including Mn, Ni, Cu, Zn, As, Se, Cd, Sb, and Pb, which probably originated from fossil fuel combustion, industrial metallurgical processes, and vehicle emissions (Gao et al., 2015; Zhang et al., 2015). The total concentration of crustal elements in the study area (3.4 μg/m^3) was slightly lower than that in Tianjin (3.9 μg/m^3) and Shijiazhuang (3.9 μg/m^3) but higher than Chengde (2.4 μg/m^3), and Beijing (3.1 μg/m^3) (Zhao et al., 2013); approximately accounting for 2%–3% of $PM_{2.5}$ in these cities. For anthropogenic pollution elements, the total concentration (1.6 μg/m^3 or 2% of $PM_{2.5}$) was higher than that in Tianjin, Shijiazhuang, Chengde and Beijing (1.2, 1.2, 0.5 and 0.6 μg/m^3, accounting for less than 1% of $PM_{2.5}$) (Zhao et al., 2013). These results indicated serious pollution in the study area, especially anthropogenic pollution. The element concentrations of $PM_{2.5}$ in heavily polluted days and in other days are shown in Table 2. The concentration of all elements in heavily polluted days was obviously higher than that in other days, with the average concentration of total elements 6.6 ± 3.1 and 3.8 ± 2.1 μg/m^3, respectively. Compared with the WSIIs and carbonaceous species, the elements had less contribution to $PM_{2.5}$, in which the ratios of total elements to $PM_{2.5}$ were only 1.8% and 2.8% (slight difference) and the crustal elements (*i.e.*, Mg, Al, and Fe) dominated the most abundant elements in $PM_{2.5}$, accounting for 62% and 67% in total elements in heavily polluted days and other days, respectively.

2.3. Mass reconstruction

The result of $PM_{2.5}$ mass closure during heavily polluted days and other days is shown in Fig. 3, including SIAs, organic matter (OM), crustal matter (CM), EC, other soluble ions, other elements, and other non-identified compositions. CM is calculated using the crustal species, which can be expressed as follows (Huang et al., 2014b):

$$CM = 2.2[Al] + 2.49[Si] + 1.63[Ca] + 2.42[Fe] + 1.94[Ti],$$

where Si is estimated based on the Al-to-Si ratio (0.46) (Chow et al., 2015) in $PM_{2.5}$. OM is estimated as an OC multiplied by 1.6 ± 0.2 for urban areas (Turpin and Lim, 2001). The sum of Na^+, K^+, F^-, and Cl^- concentrations and 20 concentrations of

Table 2 – Elemental concentrations of $PM_{2.5}$ in heavily polluted days and in other days.

	Heavily polluted days (n = 24)	Other days (n = 150)
Mg	506 ± 241	524 ± 458
Al	1521 ± 1112	1059 ± 718
Mn	121 ± 81	76 ± 45
Fe	1322 ± 771	1051 ± 806
Ni	7 ± 7	5 ± 4
Cu	53 ± 36	33 ± 21
Zn	1071 ± 978	598 ± 698
As	38 ± 33	18 ± 14
Se	11 ± 11	7 ± 5
Cd	12 ± 9	7 ± 6
Sb	14 ± 10	14 ± 13
Pb	291 ± 153	247 ± 170
Total elements	6556 ± 3130	3787 ± 2057
Total elements/$PM_{2.5}$ (%)	1.8 ± 0.9	2.8 ± 1.5

All units were in ng/m^3 unless otherwise noted.
Total elements: 23 elements.

elements (all elements except Al, Fe, and Ti) were calculated as other soluble ions and other elements, respectively, to avoid double counting of the composition.

The total reconstructed masses for $PM_{2.5}$ were 83% and 81% in heavily polluted days and other days, respectively. SIAs, OM, and CM were the major components of $PM_{2.5}$, accounting for 35%, 30%, and 7% in heavily polluted days and 38%, 23%, and 11% in other days, respectively. By comparison, the ratio of OM/$PM_{2.5}$ was higher in heavily polluted days (30%) than that in other days (23%), mainly due to the higher ratio of OC/$PM_{2.5}$ in the former case, particular higher SOC in polluted days. The ratio of SOC/OC in heavily polluted days (0.68) was higher than that in other days (0.58), suggesting more intense photochemical reaction in heavily polluted days. Nonetheless, the value of OM/$PM_{2.5}$ ratio in heavily polluted days was close to that in Xi'an (31%) and Guangzhou (33%), but much lower than the values in Beijing (41%) and Shanghai (48%); all four cities were under highly polluted events (Huang et al., 2014a). However, the ratio of CM/$PM_{2.5}$ was higher in other days (11%). With other ratios (*i.e.*, SO_4^{2-}, NO_3^-, NH_4^+, EC, et al. to $PM_{2.5}$), no obvious difference was evident. Therefore, high concentrations of OM (*i.e.*, OC) are more closely related to the high concentrations of $PM_{2.5}$ than other components, which should be paid more attention to lessen the serious pollution of $PM_{2.5}$.

2.4. Source apportionment of $PM_{2.5}$

Source contribution estimates (SCEs) were the main outputs of the chemical mass balance (CMB) model, which represented the fractional contribution to the ambient $PM_{2.5}$ concentration by each source profile used in the model run. Apart from SCEs, such diagnostic parameters like R^2 were also provided by the CMB as performance measures of the least square calculations (Pirovano et al., 2015). When the target values of diagnostic parameters address the requirements of CMB (USEPA, 2004) (https://www3.epa.gov/ttn/scram/models/receptor/EPA-CMB82Manual.pdf) (*i.e.*, $R^2 > 0.8$, $X^2 < 2$, 80% < mass% < 120%), the results of the source apportionment are acceptable.

In this study, CMB v8.2, which was developed by the USEPA, was used to apportion the sources of $PM_{2.5}$. Soil dust, secondary aerosol, coal combustion, biomass burning, vehicle and industrial emission were the main sources in Zhengzhou (Geng et al., 2013b). The details of these profiles will be the subject of another paper and are herein only summarized. The soil dust profile was obtained by chemical analyses of resuspended soil samples collected near the site. The biomass profile was obtained by combustion experiments in the Shenzhen Graduate School of Peking University (Wang et al., 2016b), supported by the public welfare projects from MEPPRC (201409010). The vehicle profile was obtained by a tunnel experiment in the Jingguang North Road Tunnel of Zhengzhou. The profile for secondary sulfate and nitrate was purely stoichiometric because NO_3^- and SO_4^{2-} existed as $(NH_4)_2SO_4$ and NH_4NO_3, which will be the subject of another paper. The source profile for coal combustion was obtained from a previous study (Zheng et al., 2005). The source profile for the industry was obtained from the report by Chen et al. (1994). According to hundreds of carbon and refractory material factories (http://www.zhengzhou.gov.cn/html/www/news4/20160826/281572.html), the profile for carbon and refractory material was obtained by chemical analyses of $PM_{2.5}$ sample from carbon and refractory factories in Zhengzhou. Eight

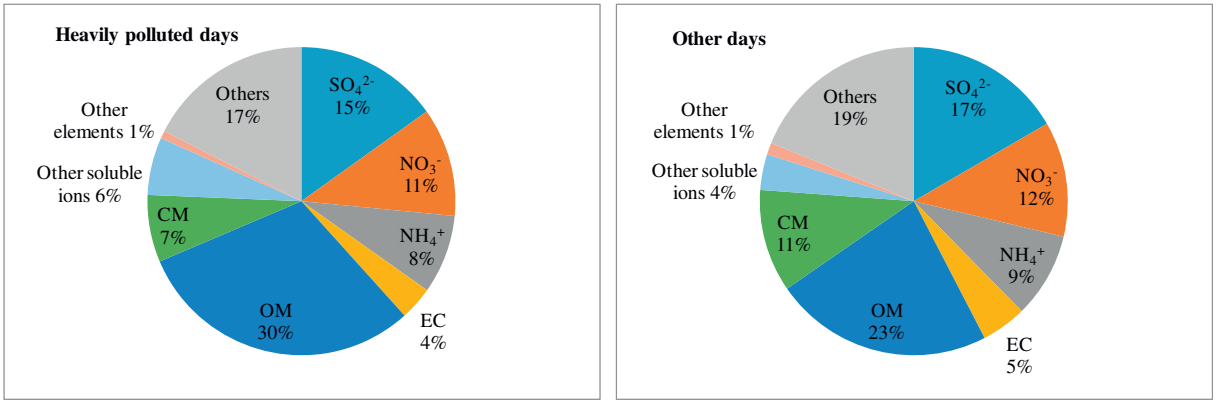

Fig. 3 – Mass closure of $PM_{2.5}$ during heavily polluted and other days.

pollution sources, including nitrate, sulfate, biomass, carbon and refractory material, coal combustion, soil dust, vehicle, and industry, were analyzed. The values of R^2, X^2, and percent mass in heavily polluted days (0.92, 0.54, and 81%, respectively) and other days (0.94, 0.47, and 115%, respectively) were all in the qualified range.

The results of source percentage contribution to $PM_{2.5}$ during heavily polluted days and other days are shown in Table 3. CMB results indicated that sulfate, coal combustion, nitrate, and biomass were the major sources in heavily polluted days, with 16%, 14%, 13%, and 12% contributions, respectively. Coal combustion, nitrate, sulfate, vehicle, and soil dust were the major sources in other days, with 27%, 20%, 18%, 15%, and 14% contributions, respectively. The results were in accordance with the results of mass reconstruction and the concentration of $PM_{2.5}$ from the same source, which was higher in heavily polluted days. The contribution of biomass burning was much higher in heavily polluted days (44 μg/m^3, 12%) than that in other days (13 μg/m^3, 9%) because most of the heavily polluted days were in autumn and winter, not only including the period of straw burning but also straw as heating and cooking fuel in the country without central heating. Although the concentration of $PM_{2.5}$ from coal combustion was higher in heavily polluted days (50 μg/m^3) than that in other days (38 μg/m^3), the impact (source contribution) was less in polluted days. Unknown sources with 19% contribution of $PM_{2.5}$ still exist, which suggests that further research is necessary for this field.

2.5. *Analysis of one haze episode*

2.5.1. *Chemical characteristics of $PM_{2.5}$*

The days during January 1–9 in 2015 were chosen for the analysis of a severe haze episode process. The concentration of $PM_{2.5}$ increased at first and reached a peak concentration on January 5, and then declined with fluctuations. All daily average concentrations of $PM_{2.5}$ during the episode process exceeded the Chinese NAAQS (daily standard: 75 μg/m^3), with the peak concentration of $PM_{2.5}$ (293 μg/m^3) exceeding beyond 2.9 times. According to the definition, three days (from January 3 to 5) were identified as heavily polluted days during the episode process with daily concentrations of $PM_{2.5}$ beyond 250 μg/m^3 and visibility lower than 3 km. The average concentrations in heavily polluted days and other days of $PM_{2.5}$, WSIIs, EC, OC, elements, and ratios of SIAs/$PM_{2.5}$, NO_3^-/SO_4^{2-}, and OC/EC are shown in Table 4.

As shown in Table 4, the average concentrations in heavily polluted days were much higher than that in other days, and the components can be classified into two categories due to the obvious or slight difference of ratios between heavily polluted days and other days. The first group includes WSIIs (133.9 ± 21.0), SIAs (101.7 ± 24.6), and NO_3^- (44.1 ± 17.9 μg/m^3), accounting for 50% ± 5%, 38% ± 8%, and 16% ± 6% of $PM_{2.5}$ in heavily polluted days, which were much higher than that (59.4 ± 13.8, 41.9 ± 12.5, and 14.2 ± 6.7 μg/m^3, accounting for 40% ± 6%, 28% ± 6%, and 9% ± 3% of $PM_{2.5}$), respectively. The obvious difference of the ratio of NO_3^-/$PM_{2.5}$ was strongly relevant to the difference of the ratio of SIAs/$PM_{2.5}$ and WSIIs/$PM_{2.5}$. The ratios of NO_3^-/SO_4^{2-} and OC/EC also have a conspicuous disparity between heavily polluted days (1.35 ± 0.49 and 2.8 ± 1.2) and

Table 3 – Source percentage contribution to $PM_{2.5}$ during heavily polluted and other days by chemical mass balance.

Source name	Source contributions (%)	
	Heavily polluted days	Other days
Nitrate	13	20
Sulfate	16	18
Biomass	12	9
Carbon and refractory material	2	2
Coal combustion	14	27
Soil dust	8	14
Vehicle	7	15
Industry	8	9

Table 4 – Average concentrations of $PM_{2.5}$, WSIIs, EC, OC, elements, and ratios of SIAs/$PM_{2.5}$, NO_3^-/SO_4^{2-}, and OC/EC during the episode event.

	Heavily polluted days (n = 3)	Other days (n = 6)
$PM_{2.5}$	268 ± 22	150 ± 31
WSIIs		
SO_4^{2-}	32.1 ± 2.3	15.1 ± 2.8
NO_3^-	44.1 ± 17.9	14.2 ± 6.7
NH_4^+	25.5 ± 4.7	12.6 ± 3.4
SIAs	101.7 ± 24.6	41.9 ± 12.5
Other soluble ions	32.2 ± 4.7	17.6 ± 3.2
WSIIs	133.9 ± 21.0	59.4 ± 13.8
Carbon		
OC	60.4 ± 20.4	32.2 ± 6.7
EC	24.7 ± 12.7	16.3 ± 4.4
TC	85.1 ± 27.7	48.5 ± 10.9
Elements		
Crustal elements	1.6 ± 0.4	1.1 ± 0.4
Total elements	3.3 ± 0.6	2.3 ± 0.8
Ratios		
SO_4^{2-}/$PM_{2.5}$ (%)	12 ± 0	10 ± 2
NO_3^-/$PM_{2.5}$ (%)	16 ± 6	9 ± 3
NH_4^+/$PM_{2.5}$ (%)	9 ± 1	8 ± 2
SIAs/$PM_{2.5}$ (%)	38 ± 8	28 ± 6
WSIIs/$PM_{2.5}$ (%)	50 ± 5	40 ± 6
OC/$PM_{2.5}$ (%)	22 ± 6	22 ± 5
EC/$PM_{2.5}$ (%)	9 ± 5	11 ± 3
TC/$PM_{2.5}$ (%)	31 ± 8	33 ± 8
NO_3^-/SO_4^{2-}	1.35 ± 0.49	0.91 ± 0.32
OC/EC	2.8 ± 1.2	2.0 ± 0.4
Crustal elements/$PM_{2.5}$ (%)	0.6 ± 0.2	0.7 ± 0.2
Total elements/$PM_{2.5}$ (%)	1.2 ± 0.2	1.5 ± 0.3

Heavily polluted days: from January 3 to January 5.
Other days: from January 1 to January 2 and January 6 to January 9.
SIAs: SO_4^{2-}, NO_3^-, NH_4^+.
Other soluble ions: Na^+, K^+, Mg^{2+}, Ca^{2+}, F^- and Cl^-.
WSIIs: 9 water soluble inorganic ions; $PM_{2.5}$: particular matter with an aerodynamic diameter < 2.5 μm; EC: elemental carbon; OC: organic carbon; SIAs: secondary inorganic aerosols; TC: total carbon.
Crustal elements: Mg, Al, Fe and Ti.
Total elements: 23 elements.
All units were μg/m^3 unless otherwise noted.

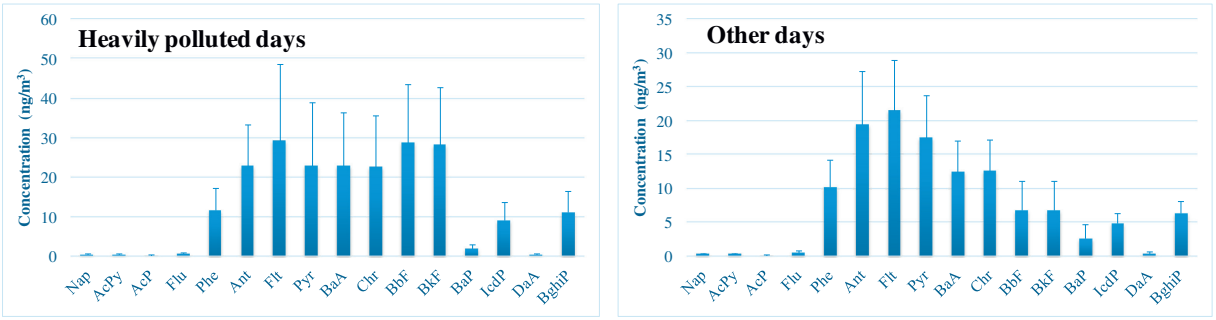

Fig. 4 – Concentrations of 16 PAHs in $PM_{2.5}$ during heavily polluted and other days. PAHs: polycyclic aromatic hydrocarbons; $PM_{2.5}$: particular matter with an aerodynamic diameter < 2.5 μm.

other days (0.91 ± 0.32 and 2.0 ± 0.4). This result was due to vehicles with low speed (because of poor visibility) in heavily polluted days, generating a considerable amount of NO_x emissions, thereby resulting in the high NO_3^- concentration. In addition, the value of OC/EC (Liu et al., 2016) indicates the presence of SOC from the photochemical reaction in heavily polluted days. The second group includes SO_4^{2-}, NH_4^+, other soluble ions, OC, EC, and crustal elements, in which the concentrations were higher with the increasing concentration of $PM_{2.5}$; however, the variation of the ratio was small. The ratios of secondary components (*i.e.*, SO_4^{2-} and NH_4^+) were notably high in heavily polluted days, whereas the value of $EC/PM_{2.5}$ was low. EC is mostly emitted from primary combustion (Yin et al., 2012); therefore, secondary pollution plays a considerable role in heavily polluted days. There are several similar results obtained from Tables 4 and 1; thus, a detailed analysis was not provided for the results of this study.

PAHs, products of incomplete combustion from various sources, such as fossil fuel combustion and biomass burning (Li et al., 2012), ubiquitously existing in vapor and particulate phases in the atmosphere, have attracted ample concern because these are carcinogenic and mutagenic (Zhang et al., 2013a). Phe, Ant, Flt, Pyr, BaA, Chr, BbF and BkF were abundant PAHs, accounting for more than 80% of PAHs (Fig. 4) during the episode. Chr and BkF were suggested for the origin of coal combustion, and Phe, Flu, Pyr, BghiP, and IcdP were proposed for the existence of motor vehicles emissions (Zhang et al., 2013a), which indicated that coal combustion and motor vehicle emissions had a considerable effect on PAHs in $PM_{2.5}$ during the episode in Zhengzhou. Average concentrations and molecular diagnostic parameters of PAHs are shown in Table 5. The total concentrations of PAHs were 214 ± 117 and 123 ± 33 ng/m^3, including 2–3 rings 14 ± 6 and 11 ± 4 ng/m^3, 4 rings 121 ± 72 and 84 ± 29 ng/m^3, and 5–6 rings 79 ± 41 and 28 ± 10 ng/m^3 in heavily polluted days and other days, respectively, accounting for approximately 0.1% of $PM_{2.5}$. The mean concentration of Carcinogenic PAHs (CANPAHs), including BaA, BbF, BkF, BaP, Chr, DaA and IcdP, was 114 ± 62 ng/m^3 (53% of PAHs) during heavily polluted days, which was much higher than that during other days (39 ± 16 ng/m^3, 32% of

Table 5 – Average concentrations and molecular diagnostic parameters of PAHs in $PM_{2.5}$ during the episode event.

Species	Heavily polluted days (n = 3)	Other days (n = 6)	Toxic Equivalent Quantity (TEQ) (Heavily polluted days)	TEQ (Other days)
$PM_{2.5}$ (μg/m^3)	268 ± 22	150 ± 31		
∑2–3 rings	14 ± 6	11 ± 4	1.36E−02	1.15E−02
∑4 rings	121 ± 72	84 ± 29	2.80E+00	1.63E+00
∑5–6 rings	79 ± 41	28 ± 10	9.21E+00	4.95E+00
∑PAHs	214 ± 117	123 ± 33	1.20E+01	6.59E+00
CANPPAHs	114 ± 62	39 ± 16	1.16E+01	6.28E+00
COMPAHs	177 ± 101	92 ± 23	1.13E+01	5.99E+00
∑PAHs/$PM_{2.5}$ (%)	0.1 ± 0.0	0.1 ± 0.0		
CANPPAHs/∑PAHs	0.53 ± 0.06	0.32 ± 0.12		
COMPAHs/∑PAHs	0.82 ± 0.05	0.75 ± 0.04		
IcdP/BghiP	0.85 ± 0.05	0.79 ± 0.01		
IcdP/(IcdP + BghiP)	0.46 ± 0.01	0.44 ± 0.01		

Heavily polluted days: from January 3 to January 5.
Other days: from January 1 to January 2 and January 6 to January 9.
2–3 rings: Nap, AcPy, AcP, Flu and Phe.
4 rings: Ant, Flt, Pyr, BaA and Chr.
5–6 rings: BbF, BkF, BaP, IcdP, DaA and BghiP.
CANPAHs (Carcinogenic PAHs): BaA, BbF, BkF, BaP, Chr, DaA and Icdp.
COMPAHs (Combustion-derived PAHs): Flt, Pyr, BaA, Chr, BbF, BkF, BaP, IcdP and BghiP.
Toxic equivalency factor for individual PAHs was proposed by Nisbet and Lagoy (1992).
All concentration units were in ng/m^3 unless otherwise noted.

PAHs), thereby indicating that CANPAHs are extremely harmful to human health with heavy pollution occurrence. Additionally, daily concentrations of BaP varied from 1 to 6 ng/m^3, with the concentrations in three days exceeding the Chinese NAAQS (2.5 ng/m^3), suggesting a potential health risk. Combustion-derived PAHs (COMPAHs), including Flt, Pyr, BaA, Chr, BbF, BkF, BaP, IcdP, and BghiP, were 177 ± 101 and 92 ± 23 ng/m^3, with the ratios of COMPAHs to ∑PAHs 0.82 ± 0.05 and 0.75 ± 0.04 in heavily polluted days and other days, thereby indicating that extensive combustion activities are the main sources of PAHs in the study area.

In addition, the diagnostic ratio analysis of PAHs was used to identify potential sources (Slezakova et al., 2013). From Table 5, the mean IcdP/(IcdP + BghiP) ratios (0.46 ± 0.01 and 0.44 ± 0.01) both below 0.5 (Yunker et al., 2002) indicated that PAHs were influenced by engine fuel combustion. Moreover, according to the previous results (approximately 0.4 for gasoline engines, and 1.0 for diesel engines) (Zhang et al., 2013a), the average values of IcdP/BghiP (0.85 ± 0.05 and 0.79 ± 0.01) also indicated that PAHs originated from vehicle emissions.

The toxicity of PAHs on health can be evaluated based on the toxic equivalency factor (TEF) multiplied by the individual PAH concentrations to convert PAH concentrations into BaP equivalency concentrations (BaPeq) (Zhang et al., 2013a). As shown in Table 5, the total BaPeq concentration (12 ng/m^3) in heavily polluted days was much higher than that in other days (7 ng/m^3), indicating PAHs in heavily polluted days with a higher health risk.

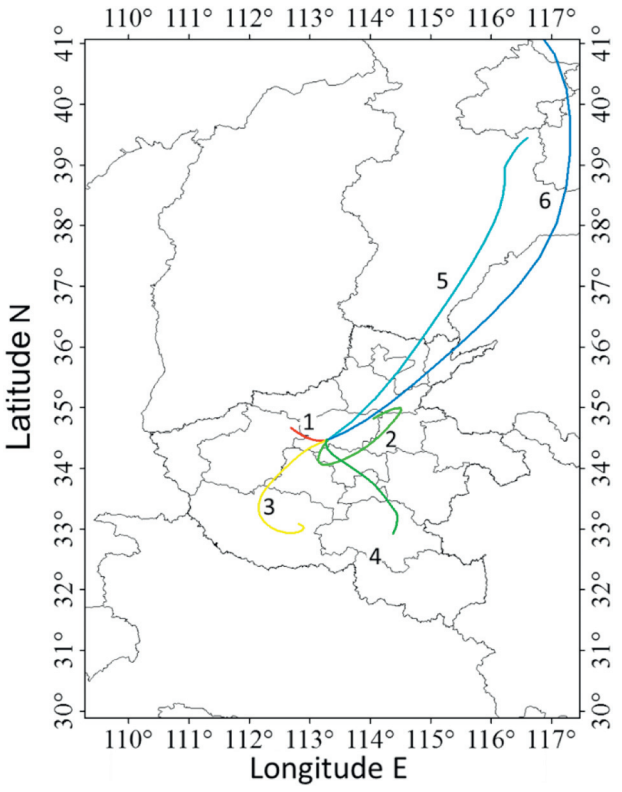

Fig. 5 – The 24-hr backward trajectories of air masses arriving in Zhengzhou at 500 m from January 1–6.

2.5.2. Back trajectory analysis

The Hybrid Single-Particle Lagrangian Integrated Trajectory (HYSPLIT) model is an effective tool used to explain the probable way, including how, when, and where potential pollutants are transported, dispersed, and deposited. Global Data Assimilation System data from the Air Resources Laboratory (data collected from the National Oceanic and Atmospheric Administration, http://ready.arl.noaa.gov/HYSPLIT.php) were used in the HYSPLIT_4 transport model to describe the airflow trajectory and the potential regional pollutant transport during the heavy pollution episode, thus showing the effect of the surrounding polluted area on our monitoring station (34°48′ N, 113°31′ E). The backward trajectory was performed to analyze the origin and direction of the air parcels affecting the air quality in the study region.

In Fig. 5, 24-hr backward trajectory lines from 1 to 6 represent air parcels arriving in our research area from January 1 to January 6, respectively at an altitude of 500 m above ground level. From January 1–4, the air mass pathway mostly came from other adjacent regions in Henan province, and the short trajectory lines proved that the regional pollution sources were close to our research area (Shen et al., 2015). Between January 5–6, lengthy movement of air mass pathway mostly came from the northeast direction weakening the stability of the atmosphere and diluting the heavy pollution condition in our research area. Thus, transport plays a significant role in increasing $PM_{2.5}$ level in the study area. The transport phenomenon is further reflected by the high $PM_{2.5}$ concentrations in adjacent regions (January 1–4) where data were retrieved from the national monitoring network (http://www.cnemc.cn/). On January 5, although the concentration of $PM_{2.5}$ increased, the ratio of SIAs/$PM_{2.5}$ decreased from 44% to 40% (data not shown). This may suggest that the external airflow plays an important role in increasing primary $PM_{2.5}$, especially considering the fact that air mass in line 5 pathway (Hebei province) is highly enriched with industrialized coal combustion byproducts. Finally on January 6, the atmospheric un-stability resulted in pollutants' dispersion with much lower $PM_{2.5}$ level. In brief, owing to the mixed considerable pollutants emitted from other regions which could be transported to the study area with the air masses, the pollution level of $PM_{2.5}$ in the study area was aggravated.

3. Conclusions

According to the three-year observation, the daily $PM_{2.5}$ concentrations varied from 50 to 698 μg/m^3, with the annual values (2013–2015: 191, 185, and 150 μg/m^3) all exceeding the annual Chinese NAAQS. The average concentrations of $PM_{2.5}$ were 366 ± 124 and 144 ± 50 μg/m^3 in heavily polluted days and in other days, respectively. The stricter measures should be implemented to lessen the pollution situation.

Almost all of the chemical composition concentrations in heavily polluted days were higher than that in other days. An obvious distinction was observed in the average concentration of each ion, which was much higher in heavily polluted days, with SIAs ($SO_4^{2-} > NO_3^- > NH_4^+$) accounting for more than 80% of WSIIs. The ratio of SOC/OC indicated that photochemical reactivity in heavily polluted days was more intense.

Elements had less contribution to $PM_{2.5}$ and crustal elements dominated the most abundant elements in $PM_{2.5}$. CMB results indicated that sulfate, nitrate, coal combustion and biomass were the major sources of $PM_{2.5}$ in heavily polluted days, and meanwhile coal combustion, nitrate, sulfate, vehicle, and soil dust were the main contributions to $PM_{2.5}$ in other days. It indicates that the enhanced regulatory measures for the main emission sources should be adopted to improve the air quality.

Concerning the severe haze episode from January 1–9 in 2015 with the peak $PM_{2.5}$ of 293 $\mu g/m^3$, the average ratios of WSIIs, SIAs and NO_3^- to $PM_{2.5}$ were in accordance with the average concentrations (much higher in heavily polluted days). However, the variation of the ratio of other compositions was smaller with the increase in concentrations and the value of EC/$PM_{2.5}$ was lower in heavily polluted days. It indicates that secondary pollution played a considerable role in heavily polluted days. The higher concentration of CANPAHs and the total BaPeq in heavily polluted days may indicate very harmful situation to human health. Additionally, daily concentrations of BaP in three days exceeding the Chinese NAAQS also suggest a potential health risk. The ratios of COMPAHs to ∑PAHs indicate that extensive combustion activities are the main sources of PAHs. The average values of IcdP/(IcdP + BghiP) and IcdP/BghiP indicate that PAHs were influenced by engine fuel combustion. According to back trajectory analysis, the transport contaminant from adjacent regions also provided a significant source for the accumulation of the episode and extended the duration of the pollution process.

Acknowledgments

The study was supported by the public welfare projects from MEPPRC (No. 201409010).

REFERENCES

Arimoto, R., Duce, R.A., Savoie, D.L., Prospero, J.M., Talbot, R., Cullen, J.D., et al., 1996. Relationships among aerosol constitutes from Asia and the North Pacific during PEM-West A. J. Geophys. Res. 101, 2011–2023.

Cao, J., Shen, Z., Chow, J.C., Qi, G., Watson, J.G., 2009. Seasonal variations and sources of mass and chemical composition for PM_{10} aerosol in Hangzhou, China. Particuology 7, 161–168.

Cao, J.J., Shen, Z.X., Chow, J.C., Watson, J.G., Lee, S.C., Tie, X.X., et al., 2012. Winter and summer $PM_{2.5}$ chemical compositions in fourteen Chinese cities. J. Air Waste Manage. Assoc. 62, 1214–1226.

Chen, Z., Ge, S., Zhang, J., 1994. Measurement and analysis for atmospheric aerosol particulates in Beijing. Res. Environ. Sci. 7, 1–9.

Chow, J.C., Lowenthal, D.H., Chen, L.W.A., Wang, X., Watson, J.G., 2015. Mass reconstruction methods for $PM_{2.5}$: a review. Air Qual. Atmos. Health 8, 243–263.

Gao, J., Tian, H., Cheng, K., Lu, L., Zheng, M., Wang, S., et al., 2015. The variation of chemical characteristics of $PM_{2.5}$ and PM_{10} and formation causes during two haze pollution events in urban Beijing, China. Atmos. Environ. 107, 1–8.

Geng, F.H., Hua, J., Mu, Z., Peng, L., Xu, X.H., Chen, R.J., et al., 2013a. Differentiating the associations of black carbon and fine particle with daily mortality in a Chinese city. Environ. Res. 120, 27–32.

Geng, N.B., Wang, J., Xu, Y.F., Zhang, W.D., Chen, C., Zhang, R.Q., 2013b. $PM_{2.5}$ in an industrial district of Zhengzhou, China: chemical composition and source apportionment. Particuology 11, 99–109.

Hu, Y., Bai, Z., Zhang, L., Xue, W., Li, Z., Yu, Q., Tan, Z., 2007. Health risk assessment for traffic policemen exposed to polycyclic aromatic hydrocarbons (PAHs) in Tianjin, China. Sci. Total Environ. 382, 240–250.

Huang, R.J., Zhang, Y., Bozzetti, C., Ho, K.F., Cao, J.J., Han, Y., et al., 2014a. High secondary aerosol contribution to particulate pollution during haze events in China. Nature 514, 218–222.

Huang, X.H.H., Bian, Q.J., Ng, W.M., Louie, P.K.K., Yu, J.Z., 2014b. Characterization of $PM_{2.5}$ major components and source investigation in suburban Hong Kong: a one year monitoring study. Aerosol Air Qual. Res. 14, 237–250.

Ji, D., Li, L., Wang, Y., Zhang, J., Cheng, M., Sun, Y., et al., 2014. The heaviest particulate air-pollution episodes occurred in northern China in January, 2013: insights gained from observation. Atmos. Environ. 92, 546–556.

Khan, M.F., Shirasuna, Y., Hirano, K., Masunaga, S., 2010. Characterization of $PM_{2.5}$, $PM_{2.5–10}$ and $PM_{>10}$ in ambient air, Yokohama, Japan. Atmos. Res. 96, 159–172.

Kim, B.M., Teffera, S., Zeldin, M.D., 2000. Characterization of $PM_{2.5}$ and PM_{10} in the south coast air basin of southern California. J. Air Waste Manage. Assoc. 50, 2034–2044.

Kim, K.H., Mishra, V.K., Kang, C.H., Choi, K.C., Kim, Y.J., Kim, D.S., 2006. The ionic compositions of fine and coarse particle fractions in the two urban areas of Korea. J. Environ. Manag. 78, 170–182.

Kong, S.F., Wen, B., Chen, K., Yin, Y., Li, L., Li, Q., Yuan, L., et al., 2014. Ion chemistry for atmospheric size-segregated aerosol and depositions at an offshore site of Yangtze River Delta region, China. Atmos. Res. 147, 205–226.

Li, Y.C., Yu, J.Z., Ho, S.S.H., Yuan, Z., Lau, A.K.H., Huang, X.F., 2012. Chemical characteristics of $PM_{2.5}$ and organic aerosol source analysis during cold front episodes in Hong Kong, China. Atmos. Res. 118, 41–51.

Liu, B., Song, N., Dai, Q., Mei, R., Sui, B., Bi, X., et al., 2016. Chemical composition and source apportionment of ambient $PM_{2.5}$ during the non-heating period in Taian, China. Atmos. Res. 170, 23–33.

Luo, Y.X., Zheng, X.B., Zhao, T.L., Chen, J., 2014. A climatology of aerosol optical depth over China from recent 10 years of MODIS remote sensing data. Int. J. Climatol 34, 863–870.

Meng, C.C., Wang, L.T., Zhang, F.F., Wei, Z., Ma, S.M., Ma, X., et al., 2016. Characteristics of concentrations and water-soluble inorganic ions in $PM_{2.5}$ in Handan City, Hebei province, China. Atmos. Res. 171, 133–146.

Nisbet, I.C., Lagoy, P.K., 1992. Toxic equivalency factors (TEFs) for polycyclic aromatic hydrocarbons (PAHs). Regul. Toxicol. Pharmacol. 16, 290–300.

Olson, D.A., Turlington, J., Duvall, R.M., McDow, S.R., Stevens, C.D., Williams, R., 2008. Indoor and outdoor concentrations of organic and inorganic molecular markers: source apportionment of $PM_{2.5}$ using low-volume samplers. Atmos. Environ. 42, 1742–1751.

Pateraki, S., Assimakopoulos, V.D., Bougiatioti, A., Kouvarakis, G., Mihalopoulos, N., Vasilakos, C., 2012. Carbonaceous and ionic compositional patterns of fine particles over an urban Mediterranean area. Sci. Total Environ. 424, 251–263.

Pathak, R.K., Yao, X.H., Lau, A.K.H., Chan, C.K., 2003. Acidity and concentrations of ionic species of $PM_{2.5}$ in Hong Kong. Atmos. Environ. 37, 1113–1124.

Pirovano, G., Colombi, C., Balzarini, A., Riva, G.M., Gianelle, V., Lonati, G., 2015. $PM_{2.5}$ source apportionment in Lombardy (Italy): comparison of receptor and chemistry-transport modelling results. Atmos. Environ. 106, 56–70.

Pope, C.R., Burnett, R.M.J.T., Calle, E., Krewski, D., Ito, K., Thurston, G., 2002. Lung cancer, cardiopulmonary mortality, and long-term exposure to fine particulate air pollution. J. Am. Med. Assoc. 287, 1132–1141.

Shen, X.J., Sun, J.Y., Zhang, X.Y., Zhang, Y.M., Zhang, L., Che, H.C., et al., 2015. Characterization of submicron aerosols and effect on visibility during a severe haze-fog episode in Yangtze River Delta, China. Atmos. Environ. 120, 307–316.

Slezakova, K., Castro, D., Delerue-Matos, C., Morais, S., Pereira, M.D.C., 2013. Impact of vehicular traffic emissions on particulate-bound pahs: levels and associated health risks. Atmos. Res. 127, 141–147.

Squizzato, S., Masiol, M., Innocente, E., Pecorari, E., Rampazzo, G., Pavoni, B., 2012. A procedure to assess local and long-range transport contributions to $PM_{2.5}$ and secondary inorganic aerosol. J. Aerosol Sci. 46, 64–76.

Tan, J., Duan, J., He, K., Ma, Y., Duan, F., Chen, Y., Fu, J., 2009. Chemical characteristics of $PM_{2.5}$ during a typical haze episode in Guangzhou. J. Environ. Sci. 21, 774–781.

Tao, M., Chen, L., Wang, Z., Ma, P., Tao, J., Jia, S., 2014. A study of urban pollution and haze clouds over northern China during the dusty season based on satellite and surface observations. Atmos. Environ. 82, 183–192.

Turpin, B.J., Lim, H.J., 2001. Species contributions to $PM_{2.5}$ mass concentrations Revisiting common assumptions for estimating organic mass. Aerosol Sci. Technol. 35, 602–610.

US EPA, 2004. EPA-CMB8.2 user manual. United States Environmental Protection Agency, Washington, DC. https://www3.epa.gov/ttn/scram/models/receptor/EPA-CMB82Manual.pdf.

Wang, Y., Zhuang, G.S., Tang, A.H., Yuan, H., Sun, Y.L., Chen, S., et al., 2005. The ion chemistry and the source of $PM_{2.5}$ aerosol in Beijing. Atmos. Environ. 39, 3771–3784.

Wang, H., An, J., Shen, L., Zhu, B., Pan, C., Liu, Z., et al., 2014a. Mechanism for the formation and microphysical characteristics of submicron aerosol during heavy haze pollution episode in the Yangtze River Delta, China. Sci. Total Environ. 490, 501–508.

Wang, H., Xu, J., Zhang, M., Yang, Y., Shen, X., Wang, Y., et al., 2014b. A study of the meteorological causes of a prolonged and severe haze episode in January 2013 over central-eastern China. Atmos. Environ. 98, 146–157.

Wang, J., Li, X., Jiang, N., Zhang, W., Zhang, R., Tang, X., 2015. Long term observations of $PM_{2.5}$-associated PAHs: comparisons between normal and episode days. Atmos. Environ. 104, 228–236.

Wang, J., Li, X., Zhang, W.K., Jiang, N., Zhang, R.Q., Tang, X.Y., 2016a. Secondary $PM_{2.5}$ in Zhengzhou, China: chemical species based on three years of observations. Aerosol Air Qual. Res. 16, 91–104.

Wang, Y., Hu, M., Wang, Y., Qin, Y., Chen, H., Zeng, L., et al., 2016b. Characterization and influence factors of $PM_{2.5}$ emitted from crop straw burning. Acta Chim. Sin. 74, 356–362.

Xu, L., Chen, X., Chen, J., Zhang, F., He, C., Zhao, J., Yin, L., 2012. Seasonal variations and chemical compositions of $PM_{2.5}$ aerosol in the urban area of Fuzhou, China. Atmos. Res. 104, 264–272.

Xu, H., Cao, J., Chow, J.C., Huang, R.J., Shen, Z., Chen, L.W., et al., 2016. Inter-annual variability of wintertime $PM_{2.5}$ chemical composition in Xi'an, China: evidences of changing source emissions. Sci. Total Environ. 545, 546–555.

Yang, Y., Liu, X., Qu, Y., Wang, J., An, J., Zhang, Y., et al., 2015. Formation mechanism of continuous extreme haze episodes in the megacity Beijing, China, in January 2013. Atmos. Res. 155, 192–203.

Yin, L., Niu, Z., Chen, X., Chen, J., Xu, L., Zhang, F., 2012. Chemical compositions of $PM_{2.5}$ aerosol during haze periods in the mountainous city of Yong'an, China. J. Environ. Sci. 24, 1225–1233.

Yunker, M.B., Macdonald, R.W., Vingarzan, R., Mitchell, R.H., Goyette, D., Sylvestre, S., 2002. PAHs in the fraser river basin: a critical appraisal of PAH ratios as indicators of PAH source and composition. Org. Geochem. 33, 489–515.

Zhang, F.W., Xu, L.L., Chen, J.S., Yu, Y.K., Niu, Z.C., Yin, L.Q., 2011. Pollution characteristics of organic and elemental carbon in $PM_{2.5}$ in Xiamen China. J. Environ. Sci. 23, 1342–1349.

Zhang, F., Xu, L., Chen, J., Chen, X., Niu, Z., Lei, T., et al., 2013a. Chemical characteristics of $PM_{2.5}$ during haze episodes in the urban of Fuzhou, China. Particuology 11, 264–272.

Zhang, R.J., Jing, J., Tao, J., Hsu, S.C., Wang, G.H., Cao, J.J., et al., 2013b. Chemical characterization and source apportionment of $PM_{2.5}$ in Beijing: seasonal perspective. Atmos. Chem. Phys. 13, 7053–7074.

Zhang, F., Wang, Z.W., Cheng, H.R., Lv, X.P., Gong, W., Wang, X.M., Zhang, G., 2015. Seasonal variations and chemical characteristics of $PM_{2.5}$ in Wuhan, central China. Sci. Total Environ. 518, 97–105.

Zhao, X., Zhang, X., Xu, X., Xu, J., Meng, W., Pu, W., 2009. Seasonal and diurnal variations of ambient $PM_{2.5}$ concentration in urban and rural environments in Beijing. Atmos. Environ. 43, 2893–2900.

Zhao, P.S., Dong, F., He, D., Zhao, X.J., Zhang, X.L., Zhang, W.Z., et al., 2013. Characteristics of concentrations and chemical compositions for $PM_{2.5}$ in the region of Beijing, Tianjin, and Hebei, China. Atmos. Chem. Phys. 13, 4631–4644.

Zheng, M., Salmon, L.G., Schauer, J.J., Zeng, L., Kiang, C.S., Zhang, Y., et al., 2005. Seasonal trends in $PM_{2.5}$ source contributions in Beijing, China. Atmos. Environ. 39, 3967–3976.

Zhou, J.B., Xing, Z.Y., Deng, J.J., Du, K., 2016. Characterizing and sourcing ambient $PM_{2.5}$ over key emission regions in China I: water-soluble ions and carbonaceous fractions. Atmos. Environ. 135, 20–30.